Journal of Structural Geology, Vol. 11, No. 8, pp. 975 to 993, 1989
Printed in Great Britain

0191-8141/89 $03.00 + 0.00
Pergamon Press plc

A comparison of the strain of crinoid columnals with that of their enclosing silty and shaly matrix on the Appalachian Plateau, New York

GERHARD OERTEL

Department of Earth and Space Sciences, University of California, Los Angeles, CA 90024, U.S.A.

TERRY ENGELDER

Department of Geosciences, Pennsylvania State University, University Park, PA 16802, U.S.A.

and

KEITH EVANS

Lamont-Doherty Geological Observatory, Palisades, NY 10964, U.S.A.

(*Received* 24 *May* 1988; *accepted in revised form* 25 *March* 1989)

Abstract—A pole-figure goniometer was used to measure the preferred orientation of the basal planes of chlorite in 87 samples from the Upper Devonian clastic rocks of the Appalachian Plateau, New York. Interpretation of the preferred orientation according to the theory of March yields an estimate of how much an element of the sediment has changed shape since deposition; this deformation can be interpreted according to three distinct models for the strain history. All begin with compaction, followed by one of three types of tectonic strain: (1) a plane strain, that conserves *bedding-plane* area by compensating for horizontal shortening with horizontal elongation at right angles; (2) one that *uniaxially* shortens a horizontal line normal to the fold axes without compensating elongation; and (3) a plane strain again, which conserves the area in the *vertical* plane containing a shortened horizontal direction by stretching it vertically. For lack of suitable names, we will simply call the three total strains type (b), (u) and (v) from the initials of the distinguishing features of their tectonic increment.

The horizontal strain components estimated from preferred orientation are compared at a number of localities with those implicit in the principal horizontal diameters of the elliptical outlines of deformed crinoid columnals found on bedding planes. Expressed for constant bedding-plane area, or type (b) total strain, the strain in the direction of greatest elongation measured by preferred orientation was found to range from no recorded strain to 0.19, with a median of 0.04. As a rule, however, the more intensive strains were recorded in shales with a fine-grained phyllosilicate content exceeding 85% by volume, in which the mean was 0.07. Deformed crinoid columnals in the same set of samples have elongations parallel to their long axes that range from 0.04 to 0.10, with a median and average of 0.07. The discrepancy between the two sets of strain measures, at least in the coarser and more permeable rock types, may either be real and caused by easier flushing of dissolved ions or may be caused by imperfect strain recording in coarse matrix materials.

INTRODUCTION

THE Upper Devonian section of the Appalachian Plateau (Fig. 1) was subject to layer-parallel shortening during the Alleghanian orogeny. Engelder & Engelder (1977) estimated a 15% shortening, mostly from their measurements of the ellipticity of originally circular crinoid columnals. They were doughnut-shaped single calcite crystals, deformed by mechanical twinning and stress solution, with the latter mechanism accounting for more than 60% of the distortion (Engelder 1979). Largely because sinks for the dissolved portion of the rock are not seen, the horizontal, layer-parallel shortening in an upper portion of the clastic section was assumed to have been by volume loss (tectonic compaction), whereas the lower portion of the clastic section was taken to have been shortened by volume-constant strain (Engelder 1985).

The Appalachian Plateau of New York and Pennsylvania is unusual for the areal extent of a clastic section which was tectonically compressed without major faulting or folding. The size of the continuously deformed rock body is a consequence of the low friction along a salt décollement on which thrusting was transferred toward the craton by more than 200 km in front of the main topographic expression of the Alleghanian orogeny (Davis & Engelder 1985, 1987). With the exception of blind thrusts just above the Silurian salt, layer-parallel shortening represents the only compensation for the slip on the décollement. Evidence for the shortening is found in the deformation of fossils in the marine Devonian section of the New York Plateau and in the cyclic sediments of the Pennsylvania Plateau (Nickelsen 1966). Average magnitude of the natural strain (natural logarithm of a principal elongation) changes by less than 10% in a 400 km long traverse along strike, from east of Binghamton, New York (Engelder & Geiser 1979) to Barnesboro, Pennsylvania (Blackmer 1987). A detailed south to north traverse from Binghamton to Syracuse suggested that layer-parallel shortening ceases only north of the pinch-out of the salt bed (Slaughter 1981).

The Upper Devonian section of the Appalachian

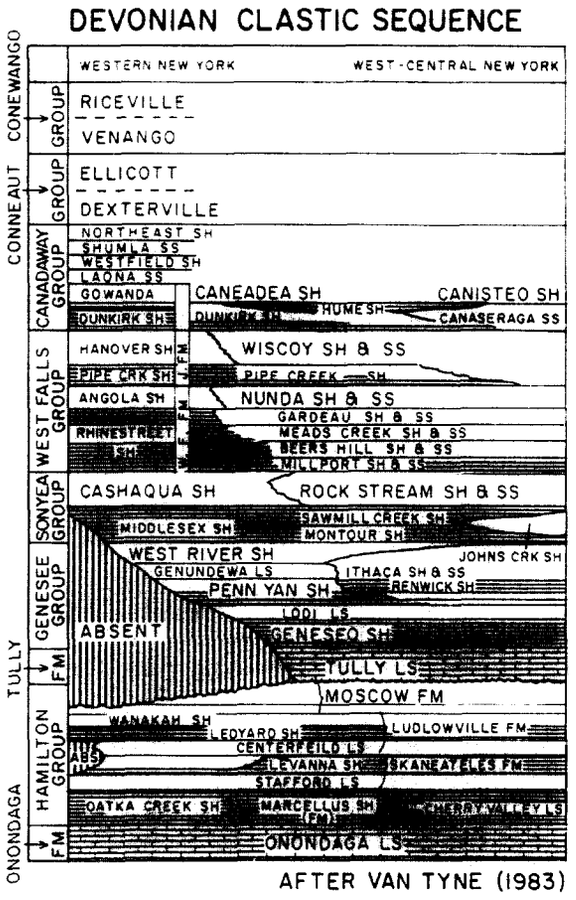

Fig. 1. Upper and Middle Devonian stratigraphy of western and west-central New York (from Van Tyne 1983). Black shale units are shown with horizontal ruling. Not to scale.

Plateau is a part of the Catskill Delta that varies in thickness from 2 km in western New York, where it is predominantly marine, to 7 km in the eastern part of the state, where fluvial deposits are common. Conodont colors indicate that between 0.5 and 1 km of sediments above those presently exposed have been eroded (Epstein *et al.* 1977), but even larger amounts of erosion are probable (e.g. Friedman 1987, Evans *et al.* in press).

Because it is so little disturbed by faulting or folding, the Appalachian Plateau is an ideal region for the study of possible discrepancies between strain indicators at all scales, from microscopic to regional. At the microscopic scale, marker inclusions in sedimentary rocks commonly differ mechanically from the matrix in which they are embedded. Because of this difference in rheological properties, markers and matrix may have different strain rates, strain histories and cumulative total strains. On the outcrop scale, beds such as the interlayered shales and siltstones typical of the Plateau differ mechanically and thus may acquire different strain. Cleavage refracting from bed to bed is indicative of this type of strain inhomogeneity (Marshak & Engelder 1985).

Previous studies of strain markers in the region have left some questions concerning the details of the strain field (Engelder & Geiser 1979). The direction of layer-parallel maximum shortening varies smoothly throughout the Upper Paleozoic section, but least strain (extension positive) measured on distorted crinoid columnals varies in extreme cases from less than −0.10 to almost −0.20 between columnals and between adjacent outcrops. We are uncertain whether the large deviations from the local mean were caused by the sampling technique, or whether the local strain actually varies between samples and outcrops. In earlier studies, Engelder and his collaborators gave little consideration to the lithology of the matrix embedding the crinoid columnals. Because the columnals are calcite inclusions in a matrix of clay and quartz grains of various sizes, strains determined from the inclusions alone may not be representative of either the bulk strain of the rock or the behavior of the Appalachian Plateau thrust sheet. Pencil cleavage, which manifests closely spaced if not necessarily penetrative cleavage in a shaly matrix (Reks & Gray 1982), certainly follows local principal strain directions, serving to indicate that much of the bulk strain affected the matrix (Engelder & Geiser 1979).

This study assesses the bulk strain on a large portion of the Appalachian Plateau by comparing the strain determined from the preferred orientation of chlorite grains in the matrix with that evident in the ellipticity of the columnals. Another impetus was the need to calibrate strains calculated from preferred orientations (Oertel 1983) against others, such as those directly measured on columnals (Engelder & Engelder 1977). The reliability of such a calibration depends, of course, on the local strain homogeneity, itself always dubious and one of the subjects of our study.

METHODS

Field sampling

For our fabric studies, 65 oriented samples were collected from 41 localities (Fig. 2). A suite of 22 additional samples came from oriented cores recovered from two wells (NY No. 1 and NY No. 4) drilled in Allegany and Steuben Counties, New York, as part of the U.S. Department of Energy's (DOE) Eastern Gas Shales Program (Cliffs Minerals Inc. 1982, Evans *et al.* in press).

Outcrop samples, many selected because of the known presence of deformed fossils, came from the seven Groups of the Upper Devonian clastic sequence between the Conewango and Hamilton, whereas only the lower five Groups from the Canadaway to the Hamilton were sampled in the DOE wells; the sampling thus includes most of the rocks forming the Catskill Delta of the central and western part of the state of New York (Fig. 1).

Pole-figure goniometer

Preferred orientations were measured on an X-ray goniometer (Wenk 1985, Oertel 1985), which permits the systematic rotation of a sample to all orientations within certain limits. The sample intercepts the X-ray beam from a diffractometer which is permanently set at

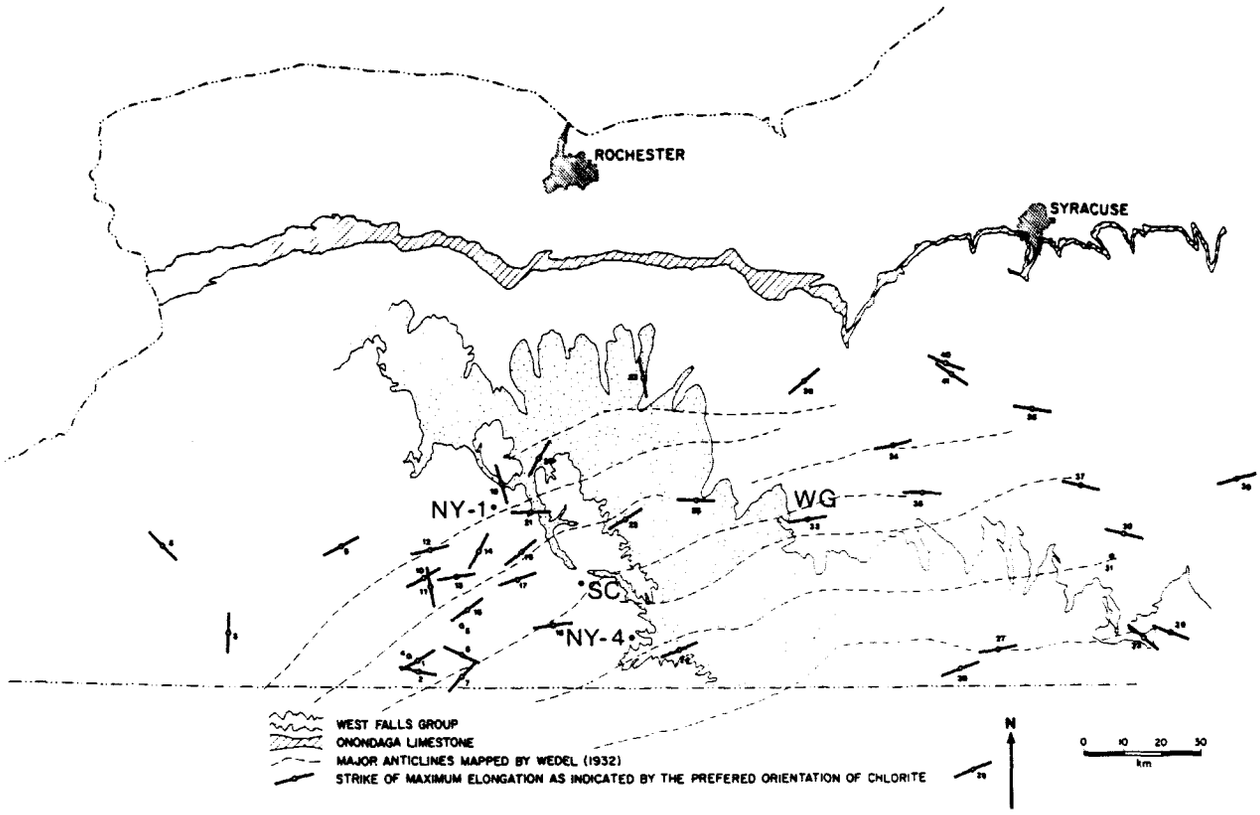

Fig. 2. Map of the Appalachian Plateau of western New York. Locations of samples (sample Nos as in the Appendix) and of wells NY No. 1 and NY No. 4, and azimuths of greatest elongation, $^{b}\varepsilon_1$, as determined from the preferred orientation of chlorite grains. WG is the location of Watkins Glen and SC that of South Canisteo.

the appropriate angle 2θ for the mineral and crystallographic plane to be investigated, chlorite (002) in our case. For any sample orientation, the intensity of X-rays diffracted from this crystallographic plane is a function of the volume of chlorite grains with basal planes in Bragg condition. The goal is to find the directions and magnitudes of principal pole densities, and then to calculate the strain from them according to the theory of March (1932).

Two orthogonal thick-sections, 0.1 mm thick and without backing, were cut from each specimen perpendicular to bedding and scanned in the transmission mode (Oertel 1983). After choosing the diffraction angle between the pencil-collimated beam and detector, X-rays are sent through the section which is rotated about an axis normal to its plane while this plane itself is gradually tilted about a fixed axis. Each rotation about the section-normal lasts 80 min, and in that time the tilt advances by 5°. As the tilt is mechanically limited to 40°, a complete scan, which lasts almost 11 h, covers an 80°-wide zone on the attitude sphere. While scanning in the reflecting mode would be an order of magnitude faster, it would preferentially sample the most disturbed region of the specimen nearest the surface. Phyllosilicate grains are particularly prone to disturbance by sample preparation and should therefore be scanned only in transmission. Intensities of diffracted X-rays are continuously recorded on a strip chart throughout the scan.

Calculation of strain from X-ray intensities

From the measured intensities of diffracted X-rays, relative principal intensities, p_i, and their directions can be determined by a procedure described by Oertel (1983, 1985). These are related to strain by the theory of March (1932). The strain determination by this method, however, is incomplete, insofar as volume changes have no influence on relative intensities.

Intensities are therefore usually normalized to represent a strain at constant volume. Its principal values are calculated by means of March's equation:

$$\varepsilon_i = p_i^{-1/3} - 1,$$

where ε_i, ordered $\varepsilon_1 > \varepsilon_2 > \varepsilon_3$, are the principal values of a strain at constant volume, expressed conventionally as $\Delta L/L_o - 1$, where L and L_o are the final and original lengths of a material line in one of the principal directions. We do not assume an actual conservation of volume but need a normalization because orientation distributions by themselves do not furnish any information about volume change. To distinguish them from other measures of strain, we shall designate as 'March strains' the direct results of calculations according to March (1932); they are listed in the Appendix as type (m) and occupy the first line of the entry for each individual outcrop.

Grain size and mineralogical composition

Many of the samples were point-counted for grain-size distribution and mineralogical composition. We counted 100 points per sample, recording grain size and minerals—quartz, calcite (usually found as a cement), opaques, lithic fragments, coarse chlorite, or fine-grained (diameter <30 μm) undifferentiated phyllosilicates (usually chlorite and/or illite).

Illite crystallinity

A measure of shale diagenesis is the transformation of clay species from the smectite group to illites. The 'crystallinity index' is a sensitive indicator of diagenetic alteration (e.g. Kubler 1968). It is customarily determined by the width of a basal-plane peak on a powder diffractogram. However, this width is also a complex function of grain size, preferred orientation of powder grains, and apparatus characteristics. Thus, the illite crystallinity index as defined by Kubler (1968) and Weaver (1967) is a somewhat uncertain measurement and should be interpreted with caution. We measured crystallinity by standard techniques.

ANALYSIS

Strain normalized to constancy of volume

Application of March's (1932) theory of strain determination from the preferred orientation of platy mineral grains assumes that clay grains were originally oriented at random, reaching the sea floor either aggregated as flocs or in fecal pellets, or later randomized by bioturbation. Uniform early distributions do exist, as shown by measurements in and around a clay–ironstone concretion (Oertel & Curtis 1972). Later the clay developed a preferred orientation of parallelism with bedding as compaction proceeded and pores collapsed, resulting in an axially symmetric pattern of pole distribution. Where a tectonic strain follows compaction or proceeds simultaneously with it, clay grains rotate so that their basal planes tend to face the direction of tectonic compression. The pattern of preferred orientation reflects the total cumulative strain from the deposition of the mudrock onward.

Any preferred orientation of phyllosilicate grains that existed before the onset of the rock's strain history must falsify strain determinations, unless the nature of the original distribution is known, a rare case. The finest clay particles are unlikely to have had such an original, sedimentary fabric, but somewhat larger grains of detrital chlorite in the sediment may have become aligned by the action of bottom currents at the time of deposition. The precise effects of grain size and current strength in developing a preferred orientation are poorly known. However, we conclude that currents probably played a role in the origin of the fabrics observed in some of our specimens, and that an original preferred orientation is probably one of the causes of irregularities in the nominal strains we calculated.

Compaction and tectonic strain

Strain that conserves volume is obviously not realistic for a sedimentary rock that must have suffered compaction, with the expulsion of connate water from the pore spaces and attendant volume loss. To estimate this loss, we must make assumptions about the later tectonic strain history. We present three end-member cases bracketing the range of possibilities for the actual local sequence of deformations. Later we will choose the most probable history.

For all three cases, we assume that the first, compactional, strain episode conserved all distances in the bedding plane, and that the only change was vertical shortening. The subsequent, tectonic, episodes are different. One tectonic strain, responsible for type (b) total strain, conserves area in the bedding plane, through a plane strain that lengthens it at right angles to the direction of tectonic shortening.

Because bedding is horizontal in the Catskill Delta and the tectonic compression acted horizontally, the strain history is coaxial. If ${}^{b}\varepsilon_i$ are the principal components of type (b) total strain (expressed conventionally as $\Delta L/L_o - 1$ and in descending order), then the assumption of area constancy in the bedding plane gives a scaling factor of $1/[(1+\varepsilon_1)(1+\varepsilon_2)]^{1/2}$, to be applied to all three principal constant-volume March type (m) stretches, $(1+\varepsilon_i)$:

$$ {}^{b}\varepsilon_i = \{(1+\varepsilon_i)/[(1+\varepsilon_1)(1+\varepsilon_2)]^{1/2}\} - 1. $$

This is the strain model we used in comparing deformation inferred from chlorite fabrics and from crinoid columnals. In this model, the compaction strain, ${}^{cb}\varepsilon_i$, that precedes tectonic deformation is:

$$ [{}^{cb}\varepsilon_i] = [0,\ 0,\ {}^{b}\varepsilon_3] $$

and is followed by a tectonic strain, ${}^{tb}\varepsilon_i$:

$$ [{}^{tb}\varepsilon_i] = [{}^{b}\varepsilon_1,\ {}^{b}\varepsilon_2,\ 0], $$

which conserves bedding plane area. The total and compaction strains of this model are listed on the second line for each entry in the Appendix, except for outcrops on which we have measurements from crinoid columnals. Then the bedding-area preserving strains from crinoids are shown in braces as the second line, with ${}^{tb}\varepsilon_i$ and ${}^{cb}\varepsilon_i$ following as the third.

A second possible strain history involves uniaxial tectonic shortening with volume loss and leads to type (u) strain. This type is suggested by the common occurrence of spaced stress-solution cleavage in the Appalachian Plateau. Probably the initial compaction under overburden had not eliminated all collapsible pore space, and thus the tectonic compression reduced line lengths in one direction in the bedding plane without compensating increases in orthogonal directions. Such a history leaves original horizontal material lines parallel to the fold axes unaltered and thus provides a scale

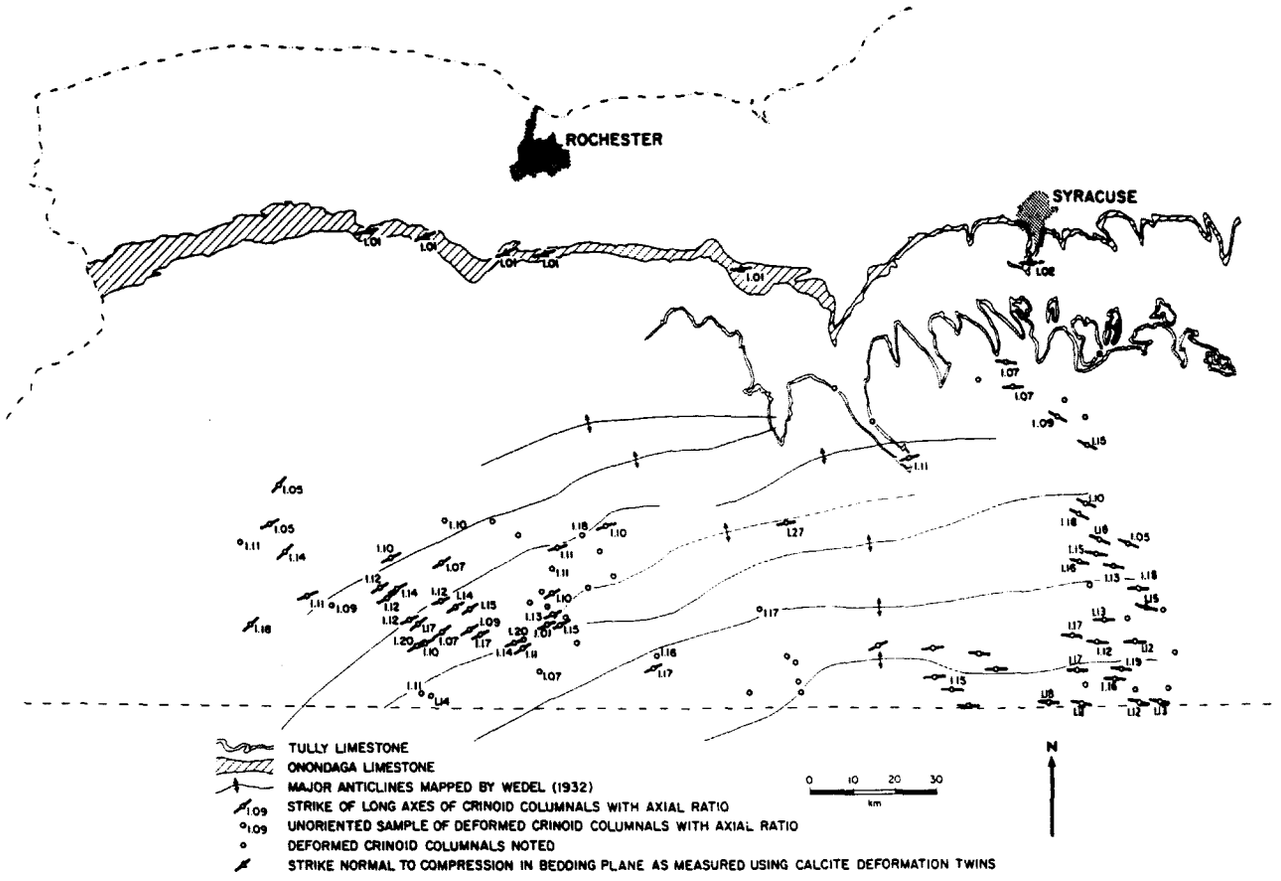

Fig. 3. Map of axial ratios of deformed crinoid columnals and of the orientation of their long axes, Devonian section of the Appalachian Plateau of western New York. The data are mostly from Engelder & Geiser (1979), with 20 data points added mainly in the eastern portion of the map.

factor of $1/(1 + \varepsilon_1)$ that must be applied to the constant-volume type (m) stretches. The components of type (u) strain, ${}^{u}\varepsilon_i$, are:

$$ {}^{u}\varepsilon_i = \{(1 + \varepsilon_i)/(1 + \varepsilon_1)\} - 1. $$

As before, the pre-tectonic compaction strain, ${}^{cu}\varepsilon_3$, equals ${}^{u}\varepsilon_3$ of the total type (u) strain:

$$ [{}^{cu}\varepsilon_i) = [0, 0, {}^{u}\varepsilon_3], $$

followed by the tectonic strain, ${}^{tu}\varepsilon_i$:

$$ [{}^{tu}\varepsilon_i] = [0, {}^{u}\varepsilon_2, 0]. $$

Type (u) strains and the corresponding pre-tectonic compactions appear in the Appendix in the second-last line for each outcrop.

The last tectonic strain type is a plane strain acting in a vertical plane and results in a type (v) total strain. The tectonic phase finds the compacted rock incompressible and shortens it horizontally, with a compensating vertical elongation, leaving area in the profile plane, and also the volume, unchanged. By assuming, as in case (u), that no elongation occurs parallel to fold axes, the final strain is the same for the two cases. What differs is the hypothetical strain path that leads to this result. By applying the same scaling factor as for (u), we calculate the type (v) strain, ${}^{v}\varepsilon_i$, as:

$$ [{}^{v}\varepsilon_i] = [{}^{u}\varepsilon_i] = [(1 + \varepsilon_i)/(1 + \varepsilon_1)] - 1. $$

Although the total strains of types (v) and (u) do not differ, we interpret their histories differently. Because the tectonic strain has a positive vertical component, ${}^{tv}\varepsilon_3$, the preceding compaction, ${}^{cv}\varepsilon_3$, must have reduced sediment thickness beyond the present state before tectonism restored it to its present total of ${}^{v}\varepsilon_3$. The plane tectonic strain, ${}^{tv}\varepsilon_i$, preserved area in the vertical plane containing the direction of greatest tectonic shortening; hence it was:

$$ [{}^{tv}\varepsilon_i] = [0, {}^{v}\varepsilon_2, \{1/(1 + {}^{v}\varepsilon_2) - 1\}], $$

where ${}^{tv}\varepsilon_2$ is necessarily negative and consequently ${}^{tv}\varepsilon_3$ positive. This implies that before tectonism the vertical compaction component, ${}^{cv}\varepsilon_3$, must have been:

$$ {}^{cv}\varepsilon_3 = \{(1 + \varepsilon_2)(1 + \varepsilon_3)/(1 + \varepsilon_1)^2\} - 1, $$

the other two components of compaction being zero. The vertical-plane total and the pre-tectonic compaction strains, type (v), are listed as the last line for each outcrop in the Appendix.

The regional strain pattern

The orientations of the principal layer-parallel deformation axes are shown in Fig. 2. Though more dispersed, the axes define the same pattern that was reported by Engelder & Geiser (1979) based on obser-

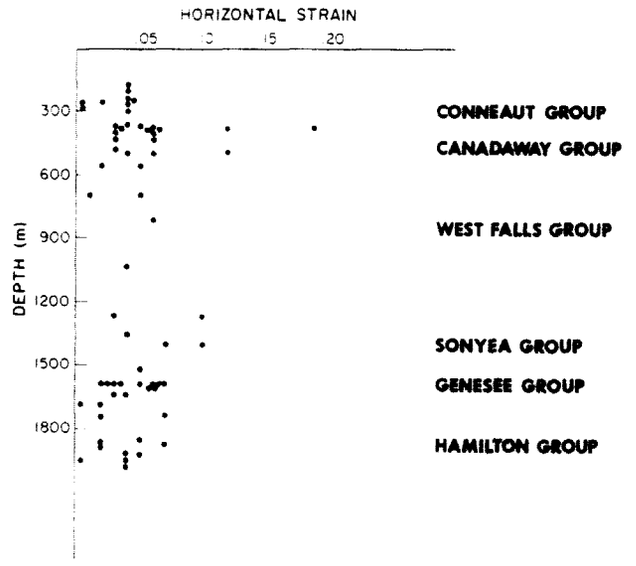

Fig. 4. Horizontal strain, ${}^{b}\varepsilon_1$, estimated from the preferred orientation of chlorite and calculated assuming conservation of area in the bedding plane vs depth of burial.

vations of both the shapes of crinoid columnals (Fig. 3) and of the orientation of pencil cleavage throughout the Appalachian Plateau.

The maximum horizontal strain measured by preferred orientation, ${}^{b}\varepsilon_1$, is shown as a function of the maximum depth of burial for each sample in Fig. 4. Burial depth was inferred from the estimates of Colton (1970), deWitt & Colton (1978), and well logs, mainly from Van Tyne & Foster (1979), with the arbitrary assumption that post-Devonian sediments were 1 km thick. Evidently, horizontal strain is independent of the depth of burial. To check for systematic regional variation in strain intensity, we divided our samples into six zones according to distance from the southeastern edge of the Appalachian Plateau. A plot of the maximum horizontal strain ${}^{b}\varepsilon_1$ vs that distance is shown in Fig. 5. The strain varies in each zone, mainly between 0.02 and 0.07, but the two variables appear to be independent of each other. This finding agrees with crinoid data of Engelder & Geiser (1979) and Slaughter (1981).

Crinoid-columnal strain

Deformed crinoid columnals are almost always found lying flat on the bedding planes. Ratios, R, of the long to the short axes of their approximately elliptical outlines were recorded. Engelder (1979) showed that the strain history of the crinoid columnals is complex and may consist of a combination of our types (u) and (v). We have calculated the simplest of our strain types, type (b), in terms of R.

The crinoid-derived horizontal strain, ${}^{cr}\varepsilon_i$, is calculated in terms of R as follows: the assumption of conservation of bedding-plane area implies the relation ship $(1 + {}^{cr}\varepsilon_1) = 1/(1 + {}^{cr}\varepsilon_2)$. Considering that R is defined as:

$$R = (1 + {}^{cr}\varepsilon_1)/(1 + {}^{cr}\varepsilon_2),$$

we have $R = (1 + {}^{cr}\varepsilon_1)^2$ and thus:

$${}^{cr}\varepsilon_1 = R^{1/2} - 1; \quad {}^{cr}\varepsilon_2 = 1/R^{1/2} - 1.$$

Columnal strains estimated in this manner are listed, where available, in braces on line 2 of each outcrop entry in the Appendix. They are best compared with the values in the line below, because both are calculated for the same assumption of constant bedding-plane area.

Average strains

Where several measurements are available at one locality, we calculated the average strain. Finite strain has non-linear aspects that make the arithmetic mean an inappropriate measure of the average. The arithmetic mean of a population of volume- or area-conserving strains, for instance, does not itself conserve volume or area (Oertel 1981). For that reason, we average strains (with one exception explained below) by first determining principal natural strains, n_i, by taking the natural logarithm of the principal stretches:

$$n_i = \ln (1 + \varepsilon_i).$$

We then refer the principal natural strains to geographic co-ordinates, $[{}^{g}x_i] = [\text{north, east, down}]$ with the help of the set of direction cosines, a_{ij}, the set of cosines of the angles from each principal co-ordinate ${}^{p}x_i$ to each geographic co-ordinate ${}^{g}x_j$. If we designate the trend angle of the long axis as α, then the matrix of direction cosines in our cases, with the vertical axis unchanged, is:

$$(a_{ij}) = \begin{bmatrix} \cos\alpha & \sin\alpha & 0 \\ -\sin\alpha & \cos\alpha & 0 \\ 0 & 0 & 1 \end{bmatrix}.$$

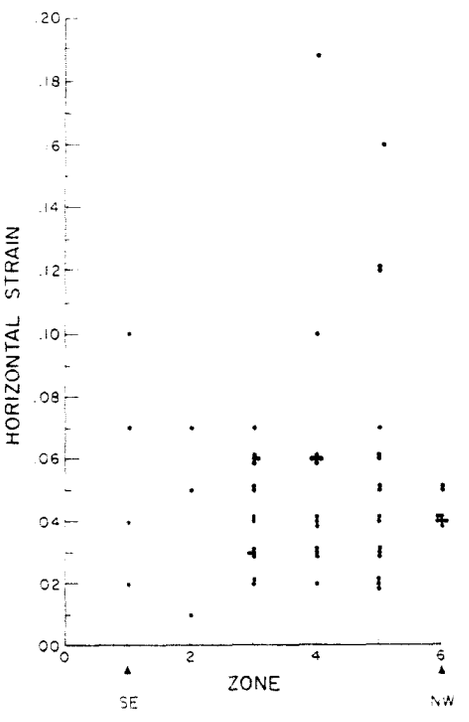

Fig. 5. Horizontal strain, ${}^{b}\varepsilon_1$, vs northwestward distance from the core of the Appalachian fold belt (in six zones).

The natural strain, ${}^{g}n_{ij}$, referred to geographic co-ordinates is then:

$$ {}^{g}n_{ij} = a_{im}a_{jn}{}^{p}n_{mn}, $$

where a repeated subscript implies summation. Arithmetic means are calculated from the populations of individual components with identical pairs of subscripts, and the eigenvalues, the principal average natural strains ${}^{p^{av}}n_i$, of the means are found, as well as their eigendirections. The natural strains are then re-converted to conventional form, ${}^{av}\varepsilon_i$, by exponentiation:

$$ {}^{av}\varepsilon_i = \exp({}^{p^{av}}n_i) - 1. $$

Comparison of crinoid and chlorite fabric strain

Complete data set. A comparison of strains estimated by the two different techniques allows a mutual calibration of the methods. It will also prove useful later when we try to balance the different weaknesses of the two sets of strain estimates against each other.

The considerations for valid averaging also apply to any other statistics on finite strain. If we wish to use a regression to visualize the fit of two different sets of strain observations, we must do so on their natural rather than conventional forms. We must also consider whether the variables to be compared are independent. Comparing strain components, we must be aware that the natural strain tensor, like all other strain tensors, is symmetrical, with identical components on opposite sides of the matrix diagonal, $n_{ij} = n_{ji}$. Additionally, if conservation of area or volume is assumed, one of the diagonal components in each strain is redundant, because it can be calculated from the others by $n_{ii} = 0$ (the repeated subscript implies summation over i). If redundant components are simultaneously used for a regression, that fact has to be taken into consideration when stating regression coefficients (Wood & Oertel

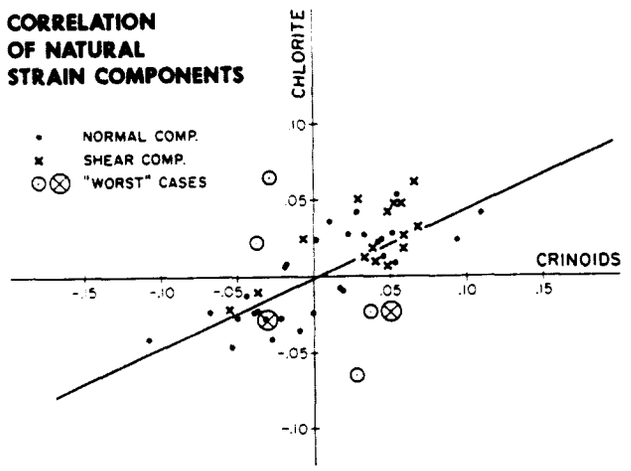

Fig. 6. Correlation of components of natural strain from preferred orientation of chlorite, ${}^{p}n_{ij}$ (ordinate), with those from crinoid columnal shape, ${}^{cr}n_{ij}$ (abscissa). Natural strain components are referred to geographic co-ordinates. Long and short normal component pairs are shown as dots, shearing components n_{12} as crosses. Heavy line–best-fit linear correlation. The worst-case results from two localities are circled.

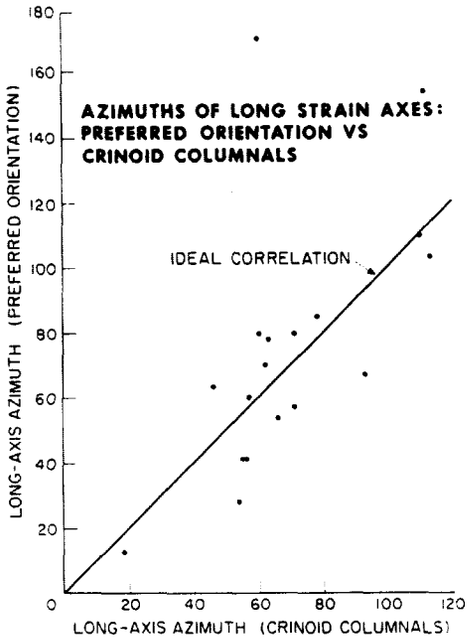

Fig. 7. Correlation of long-axis azimuth of strain from preferred orientation (ordinate) with that from crinoid columnal shape (abscissa). The solid line is not a regression line but merely represents the ideal correlation.

1980). This was done for all statistical comparisons in this paper.

Figure 6 is a plot of the two-dimensional natural strain components calculated from crinoid columnal shapes ${}^{cr}n_{ij}$ (abscissa) and from the preferred orientation of chlorite ${}^{p}n_{ij}$ (ordinate), both expressed so as to preserve area in the bedding plane (see also the Appendix). The correlation would have been the same for any other assumption made about constancy or change of area or volume, as long as it was the same for both measurements. We plot both of the diagonal 'normal' components and the off-diagonal 'shearing' component of the two kinds of strain, all referred to geographic co-ordinates.

The crinoid shapes we are using for comparison are averages from small and internally rather consistent sets of measurements on individual columnals. Mean ratios and mean azimuths of the long axes were determined by Engelder and his collaborators by calculating arithmetic means (Shimamoto & Ikeda 1976). The results are less exact than our method for strain-averaging, but checks have shown that the improvement in accuracy obtained by the more cumbersome method is not significant. We converted the mean strain findings of Engelder and collaborators into their natural strain counterparts for this comparison.

The calculated linear regression of components of the two types of natural strain, treating crinoid strain as error-free, yields a correlation coefficient of 0.62. According to Student's t-test, this pairing of observations has less than 0.001 probability of being unrelated; nevertheless, we prefer not to use slope and intercept of the regression line (heavy line in Fig. 6) to calculate equivalent strains. Six worst-case pairs, circled in Fig. 6, come from the two localities, Nos 11 and 37,

where field evidence suggests that bottom current activity may have imparted a pre-compaction preferred orientation fabric.

Eliminating the two localities from the regression improved the correlation coefficient, and the new slope for the regression line of 0.49 (not shown on Fig. 6) is more meaningful than that from the original correlation. The intercept on the abscissa was also slightly improved, to +0.003 (ideally it should be zero). Thus, on the whole, the preferred orientation in the matrix shows only half as much natural strain as the crinoids.

The azimuths of the long axes of the matrix strain are shown as a function of those of the crinoid columnals in Fig. 7. The straight line is not a regression line (lines oriented in a plane are not suitable for such a calculation. Mardia 1972) but, for comparison with the observed distribution, the ideal line for identity of the two sets is shown. Although conspicuous stray measurements are present (again associated with localities Nos 11 and 37), no significant bias can be found for axis orientation by one method or the other.

Watkins Glen detailed section. A 30 m thick section through the Ithaca Formation of the Genesee Group was studied on an outcrop at Watkins Glen (see Fig. 2, locality 33). Seven measurements appear in the Appen-

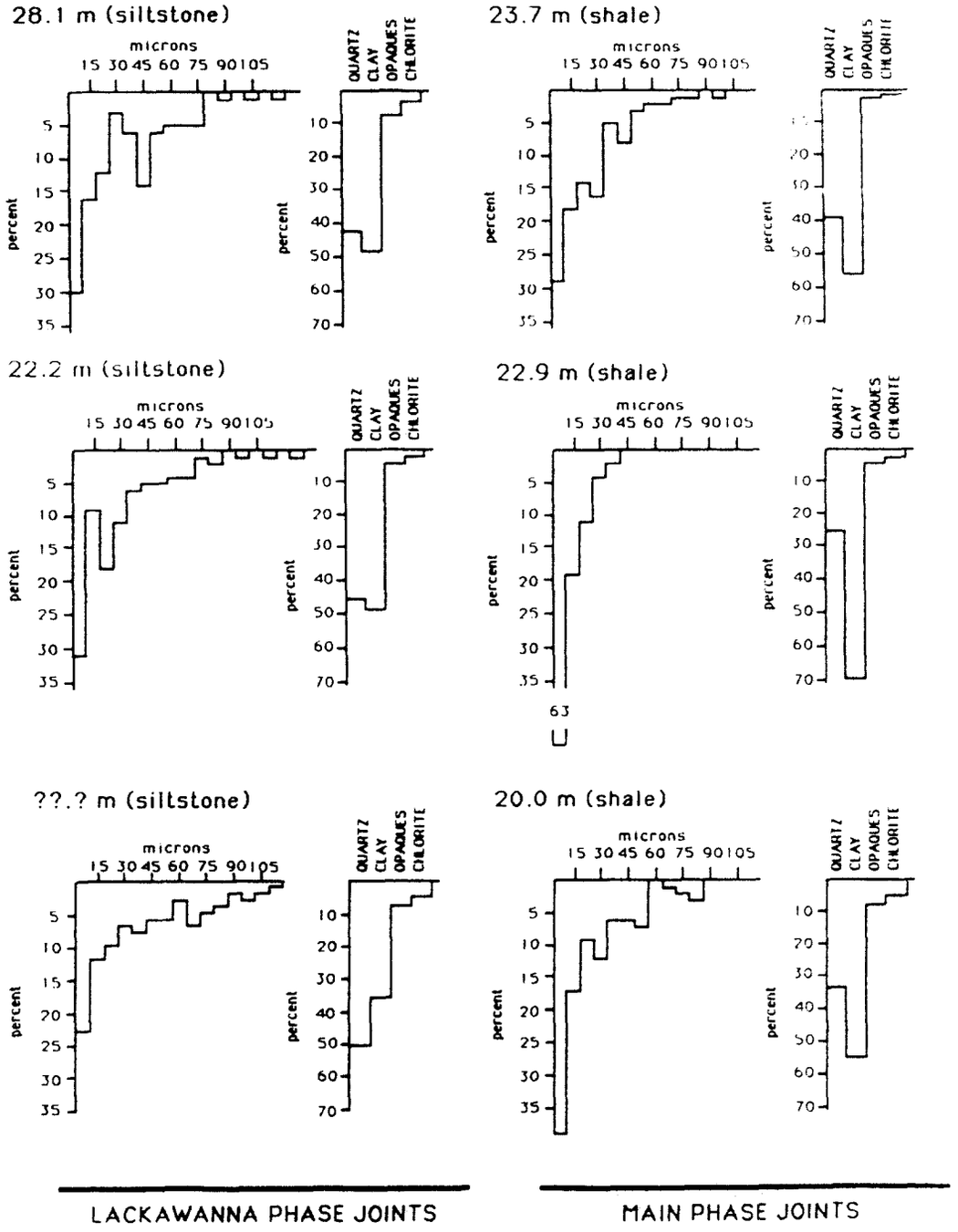

Fig. 8. Histograms of size distributions and mineralogical compositions from two classes of lithological units from the Ithaca Formation, Genesee Group, Watkins Glen, New York, arbitrarily separated into 'shales' and 'siltstones'. Localities are identified by their stratigraphic position above an arbitrary datum (see Appendix, locality No. 33). One 'siltstone' was not located with respect to the datum.

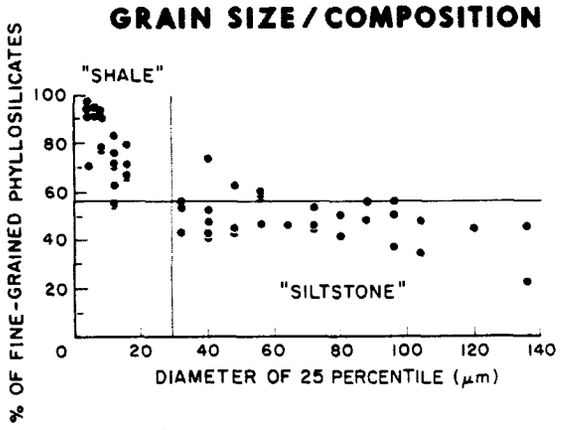

Fig. 9. Composition (percent of fine-grained phyllosilicates, including illite and all chlorite except large detrital grains) vs an aspect of the grain-size distribution (diameter, in μm, of the smallest grain larger than 75% by volume of all grains).

dix as Nos 33d–33j, with their elevations above an arbitrary stratigraphic datum shown in braces. Three more, Nos 33a–33c, have unknown positions in the stratigraphic column. Closely spaced sampling permitted comparison with other studies (Bahat & Engelder 1984, Engelder *et al.* 1987) of the strike of vertical joints as a function of lithology. Joints strike between 161 and 163° in shales but between 151 and 154° in intercalated siltstone beds. Engelder *et al.* (1987) identified this systematic discrepancy as lithology-dependent responses to distinct phases of the Alleghanian orogeny, the Lackawanna phase producing the joints at 152°, the Main phase those at 162° (Engelder & Geiser 1979). Distinction in the field between these two similar lithological types is based only on the joint development itself. As histograms from selected beds in the series show (Fig. 8), the 'siltstones' have clay to quartz ratios between 0.71 and 1.06 with more than 25% of the grains having diameters larger than 30 μm. The 'shales' have ratios between 1.21 and 4.58 with fewer than 25% of the grains exceeding 30 μm in diameter. Using this distinction between 'siltstone' and 'shale', we show in Fig. 9 the clay-size fraction in samples from throughout the Upper Devonian clastic section of the Appalachian Plateau as a function of the diameter which bounds the largest-sized 25% of the grain population (the 25th percentile).

Suspecting a possible counterpart to this joint distinction in the preferred orientation patterns, we studied the fabric strain in nine samples taken from the section. Questionably significant differences were detected by the measurements.

As shown in Fig. 10(a), compaction stated in terms of type (b) strain is more pronounced in the shales than in the siltstones. This concurs with data on compaction of the two rock types subject to the same overburden (Bond & Kominz 1984).

An apparent exception to this rule are some coarse sediments containing large detrital chlorite grains that may have settled horizontally on the sediment surface (Engelder & Oertel 1985). Of our samples, three sandstones from the Canadaway Group, Nos 13, 17 and 18, probably have such a fabric. Where preferred orientation parallel to bedding could in part be due to a depositional fabric, estimates of compaction are unreliable, but such doubts do not affect the siltstones of the Watkins Glen area.

No significant difference exists between the mean greatest principal strains, ${}^{b}\varepsilon_1$, measured in the two sets of samples (Fig. 10b). However, the horizontal principal directions of the strain in the siltstones differ noticeably from those in the shales.

Orientations of long axes of strain in the siltstones of the Watkins Glen section range from 38 to 95°, and in the shales from 76 to 99° (Fig. 10c). The long axes in the siltstones tend to be more northeasterly than those in the shales, which scatter about an easterly azimuth, and in the siltstones they are therefore in better agreement with the normal to the Lackawanna-phase joints; in the shales they are in better agreement with the normal to the Main-phase joints. Deformed crinoid columnals of the Ithaca Formation exposed in Watkins Glen are found mostly in coarser beds. Their long axes trend 71° on average and thus best agree with siltstone matrix axes and Lackawanna joint-normals. However, the numbers of samples in each of the two sets for siltstones and shales are too small for a statistical separation of strain orientations.

The combined set of samples from Watkins Glen, however, allowed us to perform some statistical tests. The average (see section on methods) principal strains

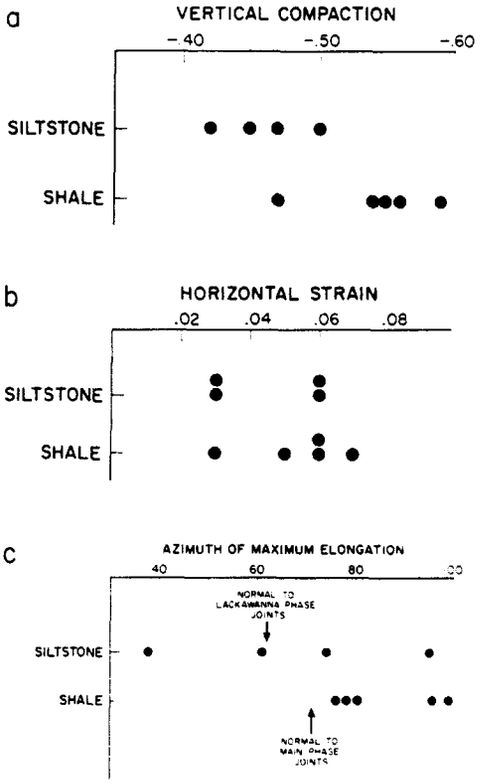

Fig. 10. Distributions for 'shales' and 'siltstones' from the Watkins Glen, New York, section, of (a) compaction, ${}^{b}\varepsilon_3$, (b) greatest elongation, ${}^{b}\varepsilon_1$, and (c) the azimuth of greatest elongation. Vertical joints in the 'shales' (Main phase, Engelder *et al.* 1987) strike 151–154°, those in the 'siltstones' (Lackawanna phase, same reference) strike 161–163°. Arrows show the directions normal to mean orientations of the two joint sets.

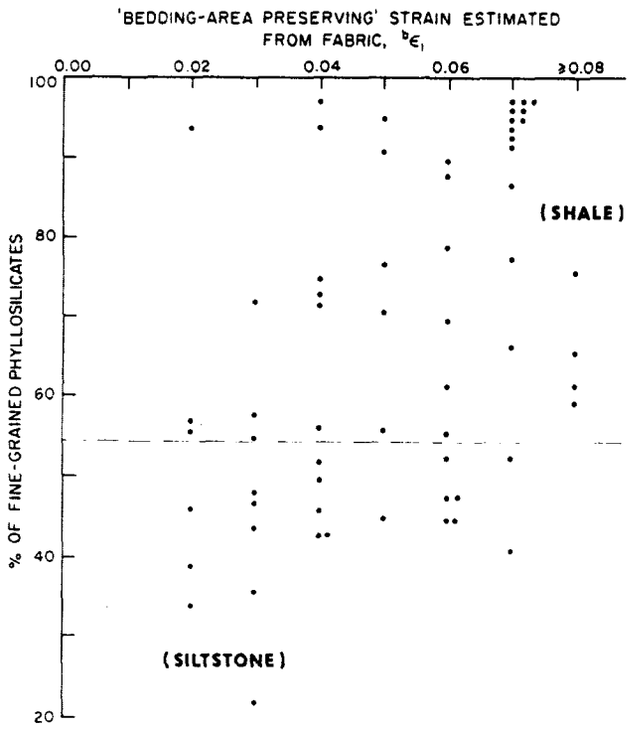

Fig. 11. Greatest elongation, $^{b}\varepsilon_1$, inferred from preferred orientation of chlorite basal planes, vs composition (volume-percent of fine-grained phyllosilicates) for the whole data set.

are [0.31, 0.22, −0.37], and the root-mean-square estimated standard deviation of these averages from expected true means is 0.016. This implies a combination of two kinds of uncertainty. First, it indicates potential deviations in any or all of the principal values. Second, considering that the uncertainty must also be understood to affect the zero-valued off-diagonal components of the strain tensor, it also implies uncertainty of orientation. Deviations from zero of 0.016 indicate potential rotations of 11° in the horizontal plane, of 2° in one of the principal vertical planes, or of 1.5° in the other. The estimated standard deviations of means we calculated for smaller populations, down to those with only two members (see Appendix), can be as large as 0.06 but are meaningless for such small populations.

Maximum elongation vs composition

The maximum fabric-inferred strain, expressed as type (b) strain $^{b}\varepsilon_1$, is plotted as a function of the relative volume fraction of fine-grained phyllosilicates (Fig. 11). Some interdependence between the two variables obviously exists; the scatter, however, appears too great to justify regression analysis. If one were to limit strain measurements to samples in which phyllosilicates are more than 90% by volume, one would find the mode of strain measurements at 0.07, close to the average measured by Engelder & Geiser (1979) on deformed crinoid columnals.

Preferred orientation and strain in samples from two wells

Strain was estimated from measurements of chlorite orientation in 22 specimens, all but one shales, from the two DOE wells NY No. 1 and NY No. 4 (localities shown in Fig. 2). The vertical sampling allows separation of the effects of burial depth from lateral variation, factors that are commingled in a regional sampling at outcrop level. We report this investigation in detail elsewhere (Evans *et al.* in press).

Type (b) strain, $^{b}\varepsilon_1$, in these wells, shown as a function of depth in Fig. 12, is essentially constant from top to bottom. This constancy contrasts with the observation by Evans *et al.* (in press) that the corresponding profile of vertical (compaction) strain, $^{b}\varepsilon_3$, declines sharply below the base of the Rhinestreet. They suggest that this break in compaction may correspond to the top of a zone which hosted abnormally high fluid pressures in the past.

For the samples from NY No. 1 with more than 85% fine-grained phyllosilicates, the average of $^{b}\varepsilon_1$ is 0.07 (in coarser samples it is commonly less but is probably not a reliable measure of strain). Within 20 km of the well, there are 19 outcrops with deformed crinoid columnals, and the average $^{cr}\varepsilon_1$ from these is 0.06. The two measures of the horizontal elongation are identical, within observational error.

Illite crystallinity

Although we have few measurements of the crystallinity index (see location map, Fig. 13), crystallinity in the Catskill Delta appears to have been affected both by depth of burial and by tectonic shortening. By stratigraphic units, the Conneaut Group has an average crystallinity index of 26, the Canadaway of 23, the West Falls of 20, and the Genesee of 18, in order of increasing crystalline perfection. Over an increase of burial depth of approximately 1500 m, diagenesis advances systematically into low anchizone metamorphism, for which the crystallinity index of 22 is usually considered the threshold.

The rocks of the region covered by the crystallinity

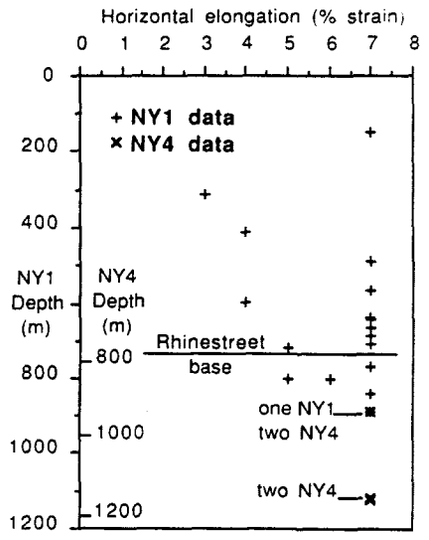

Fig. 12. Greatest elongation, $^{b}\varepsilon_1$, vs depth in samples from DOE wells NY No. 1 and NY No. 4. The lowermost data point lies about 100 m above the Salina salt.

samples were not only compacted by burial but also tectonically shortened. Comparing samples from points with approximately the same depth of burial but with extremes in the layer-parallel shortening ${}^{b}\varepsilon_2$ of -0.10 to -0.02, these are found to contrast significantly in crystallinity: Genesee Group (18) and Hamilton Group (24). Comparable contrasts in crystallinity were found in Hudson Valley carbonate rocks by Marshak & Engelder (1985).

DISCUSSION

Overburden stress

The vertical stress in the Catskill Delta was always compressive but differed locally and in time, as the pile of sediments built up. This variation in overburden stress, the concurrent temperature gradient, and a temporary development of abnormal fluid pressure (Evans *et al.* in press), caused the observed variations of both crystallinity and compaction.

Tectonic stress

The Salina Group salt below the Catskill delta probably insulated the Devonian section from significant shear stresses on horizontal planes. Consequently, whatever the state of stress, one principal stress direction must always have been vertical and the other two horizontal and essentially parallel to bedding. These horizontal stresses have varied through time in magnitude and also in orientation.

Layers of differing stiffness give the section the mechanical character of a multilayer. Thus, horizontal stresses developed in response to far-field horizontal compression must have differed layer by layer according to their stiffness. The resulting discontinuity in horizontal stress across bedding planes contrasts with the vertical principal stress which is necessarily continuous across horizontal boundaries. From the moment that rheological contrasts between beds began to develop, probably shortly after sediment accumulation, and continuing through compaction and the duration of the tectonic load, horizontal stresses must have remained discontinuous from bed to bed. This has persisted until the present (Evans *et al.* in press). The stiffest horizontal layers always carry a larger part of any horizontal load (Robin 1979).

The different orientations of joints formed during the Lackawanna and Main phases of the Alleghanian orogenic event indicate a change of principal layer-parallel stress directions (Engelder & Geiser 1979). Episodes of joint propagation provide us with glimpses of momentary stress in a possibly complex history; cumulative strain, the subject of this paper, provides the time integral over the history of strain rates.

Matrix vs crinoid-columnal strain

The correlation diagram shown in Fig. 6 suggests that

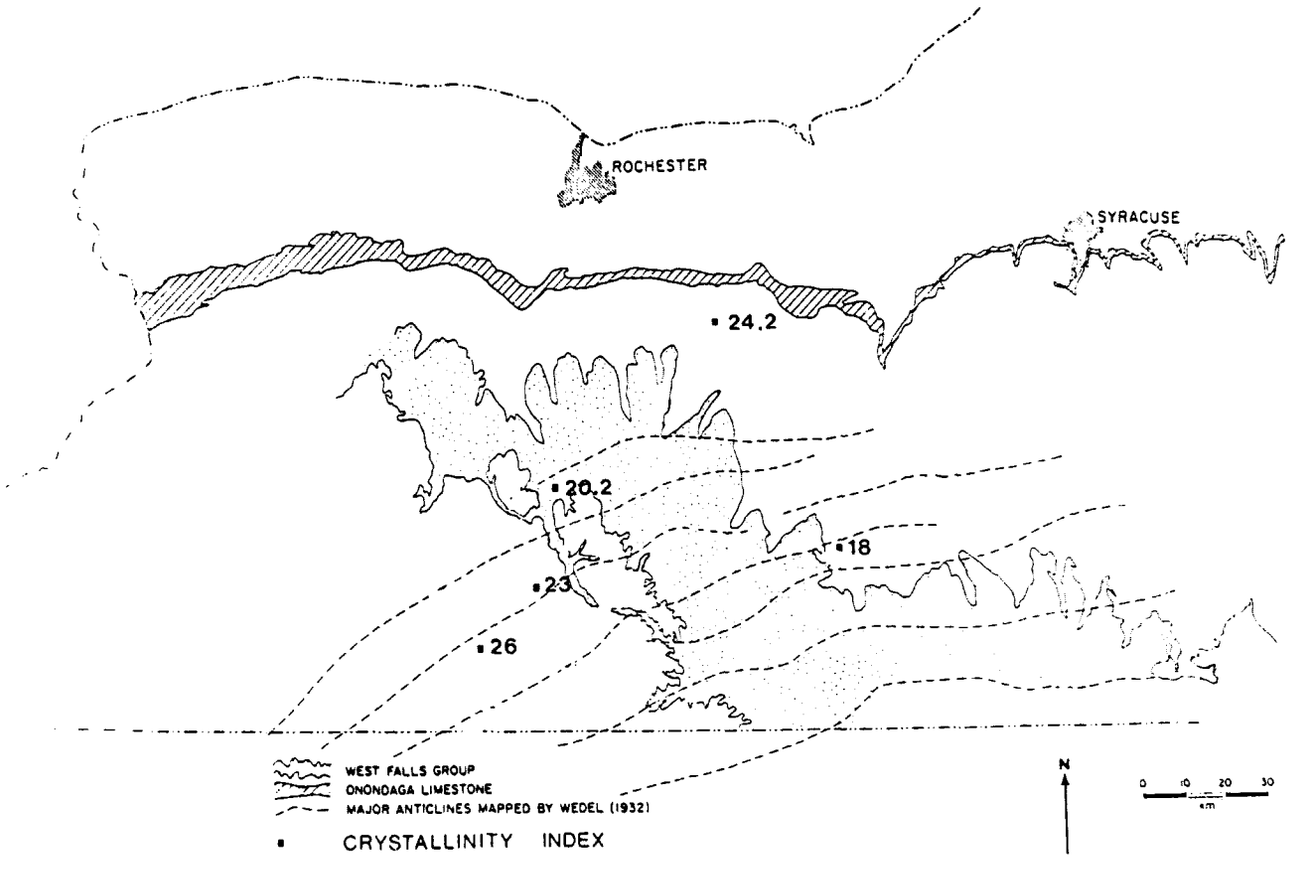

Fig. 13. Map of illite crystallinity in the Devonian section of the Appalachian Plateau of western New York.

crinoids tend to register about twice as much natural strain as does the chlorite fabric. To understand this result we have evaluated the effects of lithology on the strain recorded by the fabric. In Fig. 11 we have plotted type (b) strain, ${}^{b}\varepsilon_1$, inferred from fabric against the volume fraction of fine-grained phyllosilicates that comprise each of the specimens. Rocks composed of a greater phyllosilicate volume fraction generally record higher horizontal strains. The average value of type (b) strain, ${}^{cr}\varepsilon_1$, for crinoids is 0.07, which corresponds to the fabric strain recorded in samples consisting of more than 85% phyllosilicates. Such rocks also tend to have finer grains (Fig. 9). We conclude that shales tend to yield larger strain estimates from preferred orientation than do coarser rock types and that the fabric strain of shales approximately equals crinoid strain.

Why should coarser rock types of generally lower phyllosilicate volume fraction yield smaller estimates of fabric strain? This apparent dependence is not an artifact of the method of measuring preferred orientation. Provided the 002 chlorite peak in diffracted X-rays is sufficiently well defined, the relative amplitude of the pole densities should not depend upon total volume of chlorite present. Thus we take the less pronounced fabrics as real and requiring explanation. Strain heterogeneity on a scale smaller than the 2 mm diameter spot on the sample that is illuminated by X-rays is the most probable cause. The contribution to the local fabric from large, chlorite-rich, but little deformed domains may not be compensated by that of smaller domains that were more deformed. The apparent dependence of fabric strain on grain size we thus take as reflecting strain inhomogeneity on a microstructural scale, with relatively large volumes of phyllosilicate lying in regions which are inhibited from straining in response to macroscopic compression by nearby large grains. This inhibitory effect may become more pronounced with progressing lithification, as the cement rigidly attaches increasingly larger domains to these grains. Systematic underestimation of strain intensity by the preferred-orientation method in relatively coarse mudrocks was found before this study by Oertel & Ernst (1978) and Oertel (1980), but the required corrections were relatively small.

The imperfect recording of bulk strain by coarse rocks is independent of another expected effect, namely that large grains in mutual contact will impart to an aggregate an enhanced resistance to collapse and so make it mechanically stiffer. Strains imparted to such a bed during vertical compression should have been less than those imparted by the necessarily identical vertical stress to finer-grained neighboring beds. Our detailed study at Watkins Glen (Fig. 10a) shows systematic differences in vertical compaction strain that correlate with bed-to-bed grain-size variation (and hence mineralogic composition).

Although the mechanical contrast between coarse- and fine-grained rocks should have been equally effective for horizontal tectonic compression as for vertical compaction, this contrast must necessarily have been compensated by greater horizontal stresses in the coarser and thus stiffer beds than in the easily yielding shales. Thus, even though stiffness contrasts from bed to bed should not affect the horizontal components of the bulk strain, stress differences could lead to different stress solution on crinoids.

Could discrepancies between crinoid- and fabric-derived estimates of strain, beyond those explicable by fabric inhomogeneity, be caused by the manner in which the crinoids deformed within the matrix? As has been noted, crinoids showing the greatest ellipticity were deformed largely through stress solution around the periphery in the quadrants facing the compression direction. As there is no evidence for deposition of the dissolved material in the orthogonal quadrants, the material was evidently carried away in solution. Volume-constant deformation through twinning also occurred, but can account for at most 40% of the ellipticities. Engelder (1985) has noted that stress solution was particularly active in the sections shallower than the West Falls Group and ascribes this to fluid circulation less restricted than it may have been below.

Whether a crinoid columnal is subject to dissolution is probably due to the deviatoric compressive stress exceeding some critical value. If the steady-state stress supported by the yielding matrix around a crinoid columnal does reach this value, and if at the same time fluid circulation is not restricted, then the crinoid will begin to lose mass. Matrix strain in the vicinity of the shrinking crinoid will be enhanced to compensate for the volume decrease. As long as the matrix maintains the compressive traction on the crinoid rim, it will continue to be eroded. It follows that the strain at the fossil and in its immediate vicinity can be greater than that of the more remote matrix.

Tectonic strain

There is no evidence in the Catskill delta of either bedding-plane slip or of distributed shear parallel to bedding, which should have rotated the axis of least strain away from the bedding pole. Hence, horizontal strains must have been locally nearly uniform from top to bottom of the pile. The vertical profile of maximum horizontal strain shown in Fig. 12 samples almost the entire section remaining above the salt décollement and supports this assertion of uniformity. Assuming, further, that the principal horizontal strain orthogonal to the horizontal compression was everywhere negligibly small, the problem remains of how tectonic strain may have been partitioned between (a) layer-parallel shortening with volume loss and (b) similar shortening, but at constant volume with a compensating vertical elongation.

Engelder (1979) noted that stress solution without reprecipitation, and thus with volume loss, accounts for more than 60% of the layer-parallel shortening of crinoid columnals. The observed orientations of the mechanical twins always indicate horizontal compression combined with exclusively vertical extension. The ab-

sence of vertical compression by twinning, however, is probably not due to lack of vertical stress on the columnals but to the biologically caused orientation of the calcite crystallographic *c*-axis. This is parallel to the axial canal and tends to align vertically when the disarticulated columnals come to rest on the sea floor. Because twinning is not favored by compression parallel to *c* of a calcite crystal (Friedman & Conger 1965) crinoid columnals are unsuitable for estimates of vertical-strain components. They do, however, in contrast to preferred orientation, provide some information about volume change.

For still another reason our two kinds of strain measurement are not fully comparable: crinoid columnals are found preferentially on the surfaces of relatively coarse beds which, as discussed, differ in mechanical reaction from the finer shales. Coarse beds were less compactible, carried more of the tectonic stress, and were probably more permeable and thus favored dissolution. They also perhaps recorded late strain increments less completely than earlier ones. It is therefore important to consider the timing of stress pulses and strain increments.

Timing of compaction and tectonism

Stretching of material lines parallel to fold axes was probably either completely absent or minor. Even considering the geometric consequences of folding along an arcuate pattern of axes, lateral flow of material in the axial direction cannot have been great. Hence, we consider type 'u' or 'v' strain a better description of the strain history than type 'b'.

Volume loss comparable to that caused by stress solution on crinoid columnals (Engelder 1979, 1984) may also have been suffered by the matrix, although by a different mechanism. There is no evidence of dissolution of clastic grains in the study area, and matrix volume loss could be the effect of pore water expulsion by tectonic compression.

Layer-parallel shortening is locally homogeneous (except at the mm-scale), whereas compaction is not. This could simply be the consequence of most or all of the compaction having preceded the event responsible for the horizontal shortening, but it is not incompatible with more complex hypothetical histories. Joint distribution and calcite twinning suggest that some vertical strain occurred simultaneously with the shortening (Engelder 1985, Engelder & Oertel 1985).

Even at the cm-scale of bed thickness, the tectonic strain in the more sandy layers, and that would include most crinoid-bearing beds, may have been to a considerable extent what we designated as type (v) strain, with vertical stretching compensating for much of the horizontal compression. The greater stiffness of these beds may have acted as a stress-raiser which, in conjunction with greater permeability, facilitated columnal dissolution and internal strain. The shales, even those in the immediate vicinity, may have responded to tectonic compression with tectonic volume loss by the expulsion of remaining pore fluid. Pore fluid transport and drainage in turn would have been concentrated in the sandy interlayers, thus improving solute removal.

Geiser & Engelder (1983) suggested that the Alleghanian Orogeny in the Appalachian Plateau consisted of two distinct phases. Only where rock units have responded differently to the two tectonic pulses by registering one better than the other, can cumulative strains register such a history. A hint of such a separation exists in the difference in orientation of the strain axes between siltstone and shale of the detailed Watkins Glen section (Fig. 10c). If the siltstone beds of that section had been less lithified during the Lackawanna than during the Main phase of tectonism, the cumulative recorded strain would have principal directions nearer those of the Lackawanna principal stress axes documented by joints. In the shales, the later Main-phase pulse could have made a relatively larger contribution, thus rotating the cumulative principal strain axes clockwise. In fact, Fig. 10(c) and also the map (Fig. 3) give the impression that the cumulative strain axes are rotated clockwise beyond the azimuth of the Main-phase joints and anticlinal axes. That may mean that through time, the principal stress and strain-rate directions may have continued to rotate after the last jointing episode.

CONCLUSIONS

The orientation of maximum horizontal shortening deduced from chlorite fabrics resembles that mapped using crinoid columnals. We believe that exceptions to this rule at a few localities may reflect a fabric acquired by the coarsest phyllosilicate grains through the action of bottom currents at the time of deposition.

The magnitude of the measured lesser horizontal principal strain, expressed for convenience by a hypothetical strain history in which the tectonic strain conserved bedding plane area, was generally between -0.02 and -0.07, with the latter value found in shales with a content of fine phyllosilicates exceeding 85% by volume. The strain measured by the present shape of crinoid columnals, also expressed for constant horizontal area, lies between -0.04 and -0.10 with an average of -0.07. Either crinoid deformation overestimates strain intensity, or preferred orientation underestimates it where the rock is relatively coarse. If the sampling is restricted to shales having a fine-grained phyllosilicate fraction exceeding 85%, the estimate agrees with the average for crinoids.

Strain measured in samples from boreholes (Evans *et al.* in press), all but one of them shales, shows good internal consistency in orientation and no statistical departure in orientation or magnitude from those measured on crinoid columnals in the vicinity of the well sites.

The strains determined by the combination of both methods can be explained in terms of three distinct strain histories: each starts with compaction but ends with a different tectonic phase. The tectonic increment

can either be a plane strain that conserves area in the horizontal bedding plane (type b), or a uniaxial strain consisting only of unidirectional, layer-parallel shortening with volume loss (type u), or a plane, area-conserving strain in a vertical plane (type v), in which a layer-parallel reduction of length is compensated by vertical extension. These strain histories are not mutually exclusive, and everywhere in the study area the real history probably combined elements of all three; type (b) strain, however, which requires extension along the fold axis, probably contributed negligibly by comparison with types (u) and (v).

Acknowledgments—We thank Richard Chen for helping G. Oertel with the X-ray fabric analyses, Chuck Rine for helping T. Engelder with the grain-size sorting and composition analyses, Diane Conrad for her illite crystallinity determinations, and the late Hank Bailey of the New York State Museum in Albany for helping us obtain the samples from the DOE wells. This work was partially supported by NSF grants EAR 83-01646 (T. Engelder), EAR 80-07444 and EAR 82-18039 (G. Oertel), EPRI contract RP 2556-24 (T. Engelder) and DOE contract DE-AC21-83MC20337 (K. Evans and T. Engelder).

REFERENCES

Bahat, D. & Engelder, T. 1984. Surface morphology on cross-fold joints of the Appalachian Plateau, New York and Pennsylvania. *Tectonophysics* **104**, 299–313.

Blackmer, G. 1987. Evaluation of stress indicators and their relationship to roof fall in a coal mine in the Appalachian Plateau, Pa. Unpublished M.S. thesis, Pennsylvanian State University.

Bond, G. C. & Kominz, M. A. 1984. Construction of tectonic subsidence curves for the early Paleozoic miogeocline, southern Canadian Rocky Mountains: implications for subsidence mechanisms, age of breakup, and crustal thinning. *Bull. geol. Soc. Am.* **95**, 155–173.

Cliffs Minerals Inc. 1982. Analysis of the Devonian Shales of the Appalachian Basin. U.S. Department of Energy contract DE-AS21-80MC14693, Final Report. Springfield Clearing House, Washington, D.C.

Colton, G. W. 1970. The Appalachian basin—its depositional sequences and their geologic relationships. In: *Studies of Appalachian Geology: Central and Southern* (edited by Fisher, G. W., Pettijohn, F. J., Reed, J. C. & Weaver, K. N.). Wiley, New York, 5–47.

Davis, D. M. & Engelder, T. 1985. The role of salt in fold-and-thrust belts. *Tectonophysics* **119**, 67–88.

Davis, D. M. & Engelder, T. 1987. Thin-skinned deformation over salt. In: *Dynamical Geology of Salt and Related Structures* (edited by Lerche, I. & O'Brien, J. J.). Academic Press, Orlando, Florida, 301–338.

deWitt, W. & Colton, G. W. 1978. Physical stratigraphy of the Genesee Formation (Devonian) in western and central New York. *Prof. Pap. U.S. geol. Surv.* **1032-A**, 1–22.

Engelder, T. 1979. Mechanisms for strain within the Upper Devonian clastic sequence of the Appalachian Plateau, western New York. *Am. J. Sci.* **279**, 527–542.

Engelder, T. 1984. The role of pore water circulation during the deformation of foreland fold and thrust belts. *J. geophys. Res.* **89**, 4319–4325.

Engelder, T. 1985. Loading paths to joint propagation during a tectonic cycle: an example from the Appalachian Plateau, U.S.A. *J. Struct. Geol.* **7**, 459–476.

Engelder, T. & Engelder, R. 1977. Fossil distortion and décollement tectonics of the Appalachian Plateau. *Geology* **5**, 457–460.

Engelder, T. & Geiser, P. A. 1979. The relationship between pencil cleavage and lateral shortening within the Devonian section of the Appalachian Plateau, New York. *Geology* **7**, 460–464.

Engelder, T., Geiser, P. A. & Bahat, D. 1987. Alleghanian deformation within shales and siltstones of the Upper Devonian Appalachian Basin, Finger Lakes District, New York. *Geol. Soc. Am. Centennial Field Guide—Northeastern Section*, 113–118.

Engelder, T. & Oertel, G. 1985. Correlation between abnormal pore pressure and tectonic jointing in the Devonian Catskill Delta. *Geology* **13**, 863–866.

Epstein, A. G., Epstein, J. B. & Harris, L. D. 1977. Conodont color alteration—an index to organic metamorphism. *Prof. Pap. U.S. geol. Surv.* **995**.

Evans, K., Oertel, G. & Engelder, T. In press. Appalachian stress study 2: analysis of Devonian shale core: some implications for the nature of contemporary stress variations and Alleghanian deformation in Devonian rocks. *J. geophys. Res.*

Friedman, G. M. 1987. Vertical movements of the crust: case histories from the northern Appalachian Basin. *Geology* **15**, 1130–1133.

Friedman, M. & Conger, F. B. 1965. Dynamic interpretation of calcite twin lamellae in a naturally deformed fossil. *J. Geol.* **72**, 361–368.

Geiser, P. & Engelder, T. 1983. The distribution of layer parallel shortening fabrics in the Appalachian foreland of New York and Pennsylvania: evidence for the two non-coaxial phases of the Alleghanian orogeny. In: *Contributions to the Tectonics and Geophysics of Mountain Chains* (edited by Hatcher, R. D., Williams, H. & Zietz, I.). *Mem. geol. Soc. Am.* **158**, 161–175.

Kubler, B. 1968. Evaluation quantitative du metamorphisme par la cristallinité de l'illite. *Bull. Centre Rech. Pan. S.N.P.A.* **2**, 385–397.

March, A. 1932. Mathematische Theorie der Regelung nach der Korngestalt bei affiner Deformation. *Z. Kristallogr.* **81**, 285–297.

Mardia, K. V. 1972. *Statistics of Directional Data.* Academic Press, London.

Marshak, S. & Engelder, T. 1985. Development of cleavage in limestones of a fold-thrust belt in eastern New York. *J. Struct. Geol.* **77**, 345–359.

Nickelsen, R. P. 1966. Fossil distortion and penetrative rock deformation in the Appalachian plateau, Pennsylvania. *J. Geol.* **74**, 924–931.

Oertel, G. 1980. Strain in ductile rocks on the convex side of a folded competent bed. *Tectonophysics* **66**, 15–34.

Oertel, G. 1981. Strain estimation from scattered observations in an inhomogeneously deformed domain of rocks. *Tectonophysics* **77**, 133–150.

Oertel, G. 1983. The relationship of strain and preferred orientation of phyllosilicate grains in rocks—a review. *Tectonophysics* **100**, 413–447.

Oertel, G. 1985. Reorientation due to grain shape. In: *Preferred Orientation in Deformed Metals and Rocks: An Introduction to Modern Texture Analysis* (edited by Wenk, H. R.). Academic Press, Orlando, Florida, 259–265.

Oertel, G. & Curtis, C. D. 1972. Clay–ironstone concretion preserving fabrics due to progressive compaction. *Bull. geol. Soc. Am.* **83**, 2597–2606.

Oertel, G. & Ernst, W. G. 1978. Strain and rotation in a multilayered fold. *Tectonophysics* **48**, 77–106.

Reks, I. J. & Gray, D. R. 1982. Pencil structure and strain in weakly deformed mudstone and siltstone. *J. Struct. Geol.* **4**, 161–176.

Robin, P.-Y. 1979. Theory of metamorphic segregation and related processes. *Geochim. cosmochim. Acta* **43**, 1587–1600.

Shimamoto, T. & Ikeda, Y. 1976. Simple algebraic method for strain estimation from deformed ellipsoidal objects: 1. Basic theory. *Tectonophysics* **36**, 315–337.

Slaughter, J. 1981. Strain on the Appalachian Plateau, New York. Unpublished M.S. thesis, University of Connecticut.

Van Tyne, A. 1983. Natural gas potential of the Devonian black shales of New York. *Northeastern Geol.* **5**, 209–216.

Van Tyne, A. & Foster, B. P. 1979. Inventory and analysis of the oil and gas resources of Allegany and Cattaraugus counties, New York. Salamanca, N. Y., Southern Tier West Regional Planning and Development Board, Contract No. 77-109, N.Y.-56775-77-1-302-0609.

Weaver, C. E. 1967. Potassium, illite and the oceans. *Geochim. cosmochim. Acta* **31**, 2181–2196.

Wedel, A. A. 1932. Geologic structure of the Devonian strata of south-central New York. *Bull. New York State Mus.* **294**, 1–75.

Wenk, H. R. 1985. Measurement of pole figures. In: *Preferred Orientation of Deformed Metals and Rocks: An Introduction to Modern Texture Analysis* (edited by Wenk, H. R.). Academic Press, Orlando, Florida, 11–47.

Wood, D. S. & Oertel, G. 1980. Deformation in the Cambrian slate belt of Wales. *J. Geology* **88**, 309–326.

Wood, D. S., Oertel, G., Singh, J. & Bennett, H. F. 1976. Strain and anisotropy in rocks. *Phil. Trans. R. Soc. Lond.* **A283**, 27–42.

APPENDIX

Strain data on the New York Plateau are listed below.

1st Column: Locality number (see Fig. 2); the numbers in parentheses are averages of two or more measurements from the same locality.

2nd Column: Stratigraphic group. In parentheses the estimated thickness of overburden during Devonian time is given in meters. In braces the stratigraphic height above an arbitrary datum is given (locality 33 only).

3rd Column: Strain type: m—*March strain at constant volume*; {c} in braces—horizontal strain measured on *crinoid columnals*, expressed for constant bedding-plane area, as in type (b); b—*bedding plane strain*, i.e. compaction followed by plane tectonic strain in the bedding plane; u—*tectonic volume loss*, i.e. compaction followed by tectonic compaction: v—*tectonic vertical strain*, i.e. compaction followed by plane tectonic strain in the vertical plane.

4th–6th Columns: Three-dimensional strain components [in brackets].

7th Column: Pre-tectonic compaction (in parentheses). This is the compaction before each of the three tectonic strain types.

8th Column: Azimuth of the horizontal, longest axis of strain, as measured by *preferred orientation* or (in parentheses) on *crinoid columnals*.

Sample No.	Stratigraphic group (Devonian overburden)	Strain type	[Three-dimensional strain]			(Pre-tectonic compaction)	Azimuth of long axis (crinoid)
1	Conewango Group (260 m)	m	[0.37	0.26	−0.42]		60°
		b	[0.04	−0.04	−0.56]	(−0.56)	
		u	[0.00	−0.08	−0.58]	(−0.58)	
		v	[0.00	−0.08	−0.58]	(−0.61)	
2	(260 m)	m	[0.31	0.27	−0.40]		100°
		b	[0.02	−0.02	−0.53]	(−0.53)	
		u	[0.00	−0.03	−0.54]	(−0.54)	
		v	[0.00	−0.03	−0.54]	(−0.55)	
3	Conneaut Group (240 m)	m	[0.26	0.16	−0.32]		2°
		{c	[0.09	−0.08	—]		(46°)}
		b	[0.04	−0.04	−0.44]	(−0.44)	
		u	[0.00	−0.08	−0.46]	(−0.46)	
		v	[0.00	−0.08	−0.46]	(−0.51)	
4	(290 m)	m	[0.18	0.18	−0.28]		—
		b = u = v	[0.00	0.00	−0.39]	(−0.39)	
5	(280 m)	m	[0.23	0.23	−0.34]		—
		b = u = v	[0.00	0.00	−0.46]	(−0.46)	
6	(290 m)	m	[0.33	0.22	−0.38]		112°
		b	[0.04	−0.04	−0.51]	(−0.51)	
		u	[0.00	−0.08	−0.53]	(−0.53)	
		v	[0.00	−0.08	−0.53]	(−0.57)	
7	(300 m)	m	[0.28	0.17	−0.34]		41°
		{c	[0.05	−0.05	—]		(56°)}
		b	[0.04	−0.04	−0.46]	(−0.46)	
		u	[0.00	−0.08	−0.48]	(−0.48)	
		v	[0.00	−0.08	−0.48]	(−0.52)	
8	Canadaway Group (230 m)	m	[0.36	0.25	−0.41]		137°
		b	[0.04	−0.04	−0.55]	(−0.55)	
		u	[0.00	−0.08	−0.57]	(−0.57)	
		v	[0.00	−0.08	−0.57]	(−0.60)	
9	(260 m)	m	[0.21	0.11	−0.26]		63°
		{c	[0.07	−0.06	—]		(46°)}
		b	[0.04	−0.04	−0.36]	(−0.36)	
		u	[0.00	−0.08	−0.38]	(−0.38)	
		v	[0.00	−0.08	−0.38]	(−0.43)	
10	(390 m)	m	[0.31	0.17	−0.34]		60°
		{c	[0.06	−0.06	—]		(57°)}
		b	[0.06	−0.05	−0.47]	(−0.47)	
		u	[0.00	−0.11	−0.50]	(−0.50)	
		v	[0.00	−0.11	−0.50]	(−0.55)	
11a		m	[0.43	0.13	−0.38]		165°
		b	[0.12	−0.11	−0.51]	(−0.51)	
		u	[0.00	−0.21	−0.57]	(−0.57)	
		v	[0.00	−0.21	−0.57]	(−0.66)	
11b		m	[0.25	0.18	−0.32]		36°
		b	[0.03	−0.03	−0.44]	(−0.44)	
		u	[0.00	−0.05	−0.45]	(−0.45)	
		v	[0.00	−0.05	−0.45]	(−0.48)	
(11)	(390 m)	m	[0.31	0.17	−0.35]		172°
		{c	[0.06	−0.06	—]		(60°)}
		b	[0.06	−0.05	−0.48]	(−0.48)	
		u	[0.00	−0.11	−0.51]	(−0.51)	
		v	[0.00	−0.11	−0.51]	(−0.56)	
12a		m	[0.32	0.25	−0.39]		102°
		b	[0.03	−0.03	−0.53]	(−0.53)	
		u	[0.00	−0.06	−0.54]	(−0.54)	
		v	[0.00	−0.06	−0.54]	(−0.57)	
12b		m	[0.37	0.24	−0.41]		77°
		b	[0.05	−0.05	−0.54]	(−0.54)	
		u	[0.00	−0.10	−0.57]	(−0.57)	
		v	[0.00	−0.10	−0.57]	(−0.61)	

continued

APPENDIX *continued*

Sample No.	Stratigraphic group (Devonian overburden)	Strain type	[Three-dimensional strain]			(Pre-tectonic compaction)	Azimuth of long axis (crinoid)
(12)	Canadaway Group (380 m)	m	[0.34	0.25	−0.40]		86°
		{c	{0.05	−0.05	— }		(63°)}
		b	[0.04	−0.04	−0.54]	(−0.54)	
		u	[0.00	−0.07	−0.55]	(−0.55)	
		v	[0.00	−0.07	−0.55]	(−0.58)	
13	(400 m)	m	[0.47	0.31	−0.48]		80°
		{c	{0.07	−0.06	— }		(60°)}
		b	[0.06	−0.05	−0.63]	(−0.63)	
		u	[0.00	−0.11	−0.65]	(−0.65)	
		v	[0.00	−0.11	−0.65]	(−0.68)	
14	(375 m)	m	[0.23	0.14	−0.28]		28°
		b	[0.04	−0.04	−0.39]	(−0.39)	
		u	[0.00	−0.07	−0.42]	(−0.42)	
		v	[0.00	−0.07	−0.42]	(−0.46)	
15a		m	[0.32	0.18	−0.36]		37°
		b	[0.06	−0.05	−0.49]	(−0.49)	
		u	[0.00	−0.11	−0.52]	(−0.52)	
		v	[0.00	−0.11	−0.52]	(−0.57)	
15b		m	[0.31	0.17	−0.35]		81°
		b	[0.06	−0.05	−0.48]	(−0.48)	
		u	[0.00	−0.11	−0.50]	(−0.50)	
		v	[0.00	−0.11	−0.50]	(−0.56)	
15c		m	[0.27	0.13	−0.30]		49°
		b	[0.06	−0.05	−0.42]	(−0.42)	
		u	[0.00	−0.11	−0.45]	(−0.45)	
		v	[0.00	−0.11	−0.45]	(−0.51)	
15d		m	[0.47	0.04	−0.35]		33°
		b	[0.19	−0.16	−0.47]	(−0.47)	
		u	[0.00	−0.29	−0.56]	(−0.56)	
		v	[0.00	−0.29	−0.56]	(−0.69)	
(15)	(400 m)	m	[0.32	0.15	−0.34]		43°
		{c	{0.08	−0.08	— }		(55°)}
		b	[0.07	−0.07	−0.47]	(−0.47)	
		u	[0.00	−0.13	−0.50]	(−0.50)	
		v	[0.00	−0.13	−0.50]	(−0.57)	
16a		m	[0.26	0.15	−0.31]		42°
		b	[0.04	−0.04	−0.43]	(−0.43)	
		u	[0.00	−0.08	−0.45]	(−0.45)	
		v	[0.00	−0.08	−0.45]	(−0.50)	
16b		m	[0.27	0.14	−0.31]		54°
		b	[0.06	−0.05	−0.43]	(−0.43)	
		u	[0.00	−0.11	−0.46]	(−0.46)	
		v	[0.00	−0.11	−0.46]	(−0.52)	
(16)	(470 m)	m	[0.27	0.15	−0.31]		49°
		b	[0.05	−0.05	−0.43]	(−0.43)	
		u	[0.00	−0.09	−0.46]	(−0.46)	
		v	[0.00	−0.09	−0.46]	(−0.51)	
17	(420 m)	m	[0.38	0.30	−0.45]		70°
		{c	[0.07	−0.07	— }		(62°)}
		b	[0.03	−0.03	−0.59]	(−0.59)	
		u	[0.00	−0.06	−0.60]	(−0.60)	
		v	[0.00	−0.06	−0.60]	(−0.62)	
18	(480 m)	m	[0.44	0.35	−0.49]		80°
		{c	[0.07	−0.06	— }		(71°)}
		b	[0.03	−0.03	−0.63]	(−0.63)	
		u	[0.00	−0.06	−0.64]	(−0.64)	
		v	[0.00	−0.06	−0.64]	(−0.66)	
19	West Falls Group (470 m)	m	[0.19	0.12	−0.25]		164°
		b	[0.03	−0.03	−0.35]	(−0.35)	
		u	[0.00	−0.05	−0.37]	(−0.37)	
		v	[0.00	−0.05	−0.37]	(−0.40)	
20a		m	[0.22	0.10	−0.26]		17°
		b	[0.05	−0.05	−0.36]	(−0.36)	
		u	[0.00	−0.09	−0.39]	(−0.39)	
		v	[0.00	−0.09	−0.39]	(−0.45)	
20b		m	[0.28	0.22	−0.36]		70°
		b	[0.02	−0.02	−0.49]	(−0.49)	
		u	[0.00	−0.05	−0.50]	(−0.50)	
		v	[0.00	−0.05	−0.50]	(−0.52)	
(20)	(540 m)	m	[0.23	0.18	−0.31]		31°
		b	[0.02	−0.02	−0.43]	(−0.43)	
		u	[0.00	−0.05	−0.44]	(−0.44)	
		v	[0.00	−0.05	−0.44]	(−0.47)	

continued

APPENDIX *continued*

Sample No.	Stratigraphic group (Devonian overburden)	Strain type	[Three-dimensional strain]			(Pre-tectonic compaction)	Azimuth of long axis (crinoid)
21	West Falls Group (500 m)	m	[0.39	0.11	−0.35]		89°
		b	[0.12	−0.11	−0.48]	(−0.48)	
		u	[0.00	−0.21	−0.53]	(−0.53)	
		v	[0.00	−0.21	−0.53]	(−0.63)	
22	(800 m)	m	[0.32	0.18	−0.36]		57°
		{c	[0.05	−0.05	—]		(71°)}
		b	[0.06	−0.05	−0.48]	(−0.48)	
		u	[0.00	−0.11	−0.51]	(−0.51)	
		v	[0.00	−0.11	−0.51]	(−0.56)	
23	(1050 m)	m	[0.29	0.20	−0.36]		170°
		b	[0.04	−0.04	−0.48]	(−0.48)	
		u	[0.00	−0.07	−0.50]	(−0.50)	
		v	[0.00	−0.07	−0.50]	(−0.54)	
24a		m	[0.23	0.21	−0.33]		86°
		b	[0.01	−0.01	−0.45]	(−0.45)	
		u	[0.00	−0.02	−0.46]	(−0.46)	
		v	[0.00	−0.02	−0.46]	(−0.46)	
24b		m	[0.27	0.15	−0.31]		50°
		b	[0.05	−0.05	−0.43]	(−0.43)	
		u	[0.00	−0.10	−0.46]	(−0.46)	
		v	[0.00	−0.10	−0.46]	(−0.51)	
(24)	(750 m)	m	[0.25	0.18	−0.32]		54°
		{c	[0.05	−0.05	—]		(58°)}
		b	[0.03	−0.03	−0.44]	(−0.44)	
		u	[0.00	−0.05	−0.45]	(−0.45)	
		v	[0.00	−0.05	−0.45]	(−0.48)	
25a		m	[0.31	0.23	−0.38]		101°
		b	[0.03	−0.03	−0.51]	(−0.51)	
		u	[0.00	−0.06	−0.52]	(−0.52)	
		v	[0.00	−0.06	−0.52]	(−0.55)	
25b		m	[0.41	0.17	−0.40]		85°
		b	[0.10	−0.09	−0.53]	(−0.53)	
		u	[0.00	−0.17	−0.57]	(−0.57)	
		v	[0.00	−0.17	−0.57]	(−0.65)	
(25)	(1260 m)	m	[0.36	0.20	−0.39]		89°
		b	[0.06	−0.06	−0.52]	(−0.52)	
		u	[0.00	−0.11	−0.55]	(−0.55)	
		v	[0.00	−0.11	−0.55]	(−0.60)	
26a		m	[0.40	0.15	−0.38]		58°
		b	[0.10	−0.09	−0.51]	(−0.51)	
		u	[0.00	−0.18	−0.55]	(−0.55)	
		v	[0.00	−0.18	−0.55]	(−0.63)	
26b		m	[0.24	0.15	−0.30]		130°
		b	[0.04	−0.04	−0.41]	(−0.41)	
		u	[0.00	−0.07	−0.43]	(−0.43)	
		v	[0.00	−0.07	−0.43]	(−0.47)	
(26)	(1375 m)	m	[0.27	0.19	−0.34]		67°
		{c	[0.07	−0.07	—]		(93°)}
		b	[0.04	−0.04	−0.46]	(−0.46)	
		u	[0.00	−0.07	−0.48]	(−0.48)	
		v	[0.00	−0.07	−0.48]	(−0.52)	
27	(1375 m)	m	[0.36	0.19	−0.38]		79°
		b	[0.07	−0.07	−0.51]	(−0.51)	
		u	[0.00	−0.13	−0.55]	(−0.55)	
		v	[0.00	−0.13	−0.55]	(−0.60)	
28	(1600 m)	m	[0.37	0.20	−0.39]		66°
		b	[0.07	−0.07	−0.53]	(−0.53)	
		u	[0.00	−0.13	−0.56]	(−0.56)	
		v	[0.00	−0.13	−0.56]	(−0.61)	
29	(1840 m)	m	[0.32	0.28	−0.41]		110°
		{c	[0.06	−0.06	—]		(110°)}
		b	[0.02	−0.02	−0.55]	(−0.55)	
		u	[0.00	−0.03	−0.55]	(−0.55)	
		v	[0.00	−0.03	−0.55]	(−0.57)	
30	Sonyea Group (1930 m)	m	[0.30	0.19	−0.36]		103°
		{c	[0.08	−0.08	—]		(113°)}
		b	[0.04	−0.04	−0.48]	(−0.48)	
		u	[0.00	−0.08	−0.51]	(−0.51)	
		v	[0.00	−0.08	−0.51]	(−0.55)	
31	(1930 m)	m	[0.26	0.26	−0.37]		—
		b = u = v	[0.00	0.00	−0.50]	(−0.50)	

continued

APPENDIX *continued*

Sample No.	Stratigraphic group (Devonian overburden) {above datum}	Strain type	[Three-dimensional strain]	(Pre-tectonic compaction)	Azimuth of long axis (crinoid)
32	(1870 m)	m	[0.27 0.11 −0.29]		128°
		b	[0.07 −0.07 −0.40]	(−0.40)	
		u	[0.00 −0.13 −0.44]	(−0.44)	
		v	[0.00 −0.13 −0.44]	(−0.51)	
33a	Genesee Group	m	[0.25 0.21 −0.33]		161°
		b	[0.02 −0.02 −0.46]	(−0.46)	
		u	[0.00 −0.03 −0.47]	(−0.47)	
		v	[0.00 −0.03 −0.47]	(−0.48)	
33b		m	[0.30 0.22 −0.37]		74°
		b	[0.03 −0.03 −0.50]	(−0.50)	
		u	[0.00 −0.06 −0.51]	(−0.51)	
		v	[0.00 −0.06 −0.51]	(−0.54)	
33c		m	[0.39 0.25 −0.42]		99°
		b	[0.05 −0.05 −0.56]	(−0.56)	
		u	[0.00 −0.10 −0.58]	(−0.58)	
		v	[0.00 −0.10 −0.58]	(−0.62)	
33d	{28.1 m}	m	[0.29 0.16 −0.33]		61°
		b	[0.06 −0.05 −0.45]	(−0.45)	
		u	[0.00 −0.11 −0.48]	(−0.48)	
		v	[0.00 −0.11 −0.48]	(−0.54)	
33e	{23.7 m}	m	[0.37 0.22 −0.40]		78°
		b	[0.06 −0.05 −0.54]	(−0.54)	
		u	[0.00 −0.11 −0.56]	(−0.56)	
		v	[0.00 −0.11 −0.56]	(−0.61)	
33f	{22.9 m}	m	[0.38 0.23 −0.41]		76°
		b	[0.06 −0.05 −0.55]	(−0.55)	
		u	[0.00 −0.11 −0.57]	(−0.57)	
		v	[0.00 −0.11 −0.57]	(−0.62)	
33g	{22.2 m}	m	[0.28 0.20 −0.35]		38°
		b	[0.03 −0.03 −0.47]	(−0.47)	
		u	[0.00 −0.06 −0.49]	(−0.49)	
		v	[0.00 −0.06 −0.49]	(−0.52)	
33h	{20.0 m}	m	[0.28 0.20 −0.35]		80°
		b	[0.03 −0.03 −0.47]	(−0.47)	
		u	[0.00 −0.06 −0.49]	(−0.49)	
		v	[0.00 −0.06 −0.49]	(−0.52)	
33i	{17.0 m}	m	[0.27 0.13 −0.30]		95°
		b	[0.06 −0.06 −0.42]	(−0.42)	
		u	[0.00 −0.12 −0.45]	(−0.45)	
		v	[0.00 −0.12 −0.45]	(−0.52)	
33j	{12.5 m}	m	[0.44 0.26 −0.45]		96°
		b	[0.07 −0.07 −0.59]	(−0.59)	
		u	[0.00 −0.13 −0.61]	(−0.61)	
		v	[0.00 −0.13 −0.61]	(−0.66)	
(33)	(1600 m)	m	[0.31 0.22 −0.37]		82°
		{c	[0.13 −0.11 —]		(78°)}
		b	[0.04 −0.03 −0.50]	(−0.50)	
		u	[0.00 −0.07 −0.52]	(−0.52)	
		v	[0.00 −0.07 −0.52]	(−0.55)	
34a		m	[0.30 0.14 −0.33]		76°
		b	[0.07 −0.07 −0.45]	(−0.45)	
		u	[0.00 −0.13 −0.48]	(−0.48)	
		v	[0.00 −0.13 −0.48]	(−0.55)	
34b		m	[0.30 0.25 −0.39]		78°
		b	[0.02 −0.02 −0.52]	(−0.52)	
		u	[0.00 −0.04 −0.53]	(−0.53)	
		v	[0.00 −0.04 −0.53]	(−0.55)	
(34)	(1750 m)	m	[0.30 0.19 −0.36]		77°
		b	[0.05 −0.04 −0.48]	(−0.48)	
		u	[0.00 −0.09 −0.51]	(−0.51)	
		v	[0.00 −0.09 −0.51]	(−0.55)	
35a		m	[0.29 0.21 −0.36]		141°
		b	[0.03 −0.03 −0.49]	(−0.49)	
		u	[0.00 −0.06 −0.51]	(−0.51)	
		v	[0.00 −0.06 −0.51]	(−0.54)	
35b		m	[0.29 0.20 −0.36]		72°
		b	[0.04 −0.04 −0.48]	(−0.48)	
		u	[0.00 −0.07 −0.50]	(−0.50)	
		v	[0.00 −0.07 −0.50]	(−0.54)	
(35)	(1675 m)	m	[0.27 0.23 −0.36]		99°
		b	[0.01 −0.01 −0.49]	(−0.49)	
		u	[0.00 −0.02 −0.49]	(−0.49)	
		v	[0.00 −0.02 −0.49]	(−0.51)	

continued

APPENDIX *continued*

Sample No.	Stratigraphic group (Devonian overburden)	Strain type	[Three-dimensional strain]	(Pre-tectonic compaction)	Azimuth of long axis (crinoid)
36a		m	[0.20 0.16 −0.28]		98°
		b	[0.02 −0.02 −0.39]	(−0.39)	
		u	[0.00 −0.03 −0.40]	(−0.40)	
		v	[0.00 −0.03 −0.40]	(−0.42)	
36b		m	[0.23 0.23 −0.34]		—
		b = u = v	[0.00 0.00 −0.46]	(−0.46)	
(36)	Genese Group (1700 m)	m	[0.22 0.20 −0.31]		98°
		b	[0.01 −0.01 −0.43]	(−0.43)	
		u	[0.00 −0.02 −0.44]	(−0.44)	
		v	[0.00 −0.02 −0.44]	(−0.44)	
37a		m	[0.22 0.18 −0.31]		11°
		b	[0.02 −0.02 −0.43]	(−0.43)	
		u	[0.00 −0.03 −0.43]	(−0.43)	
		v	[0.00 −0.03 −0.43]	(−0.45)	
37b		m	[0.24 0.11 −0.27]		147°
		b	[0.05 −0.05 −0.38]	(−0.38)	
		u	[0.00 −0.10 −0.41]	(−0.41)	
		v	[0.00 −0.10 −0.41]	(−0.47)	
(37)	(1850 m)	m	[0.22 0.16 −0.29]		155°
		{c	[0.05 −0.05 —]		(111°)}
		b	[0.03 −0.03 −0.40]	(−0.40)	
		u	[0.00 −0.05 −0.42]	(−0.42)	
		v	[0.00 −0.05 −0.42]	(−0.45)	
38	(2350 m)	m	[0.26 0.24 −0.36]		80°
		b	[0.01 −0.01 −0.48]	(−0.48)	
		u	[0.00 −0.02 −0.49]	(−0.49)	
		v	[0.00 −0.02 −0.49]	(−0.50)	
39	Hamilton Group (1520 m)	m	[0.29 0.17 −0.34]		51°
		b	[0.05 −0.05 −0.46]	(−0.46)	
		u	[0.00 −0.10 −0.49]	(−0.49)	
		v	[0.00 −0.10 −0.49]	(−0.54)	
40a		m	[0.32 0.21 −0.37]		130°
		b	[0.04 −0.04 −0.50]	(−0.50)	
		u	[0.00 −0.08 −0.52]	(−0.52)	
		v	[0.00 −0.08 −0.52]	(−0.56)	
40b		m	[0.27 0.18 −0.34]		89°
		b	[0.04 −0.04 −0.46]	(−0.46)	
		u	[0.00 −0.07 −0.48]	(−0.48)	
		v	[0.00 −0.07 −0.48]	(−0.52)	
(40)	(1900 m)	m	[0.28 0.21 −0.35]		112°
		b	[0.03 −0.03 −0.48]	(−0.48)	
		u	[0.00 −0.06 −0.50]	(−0.50)	
		v	[0.00 −0.06 −0.50]	(−0.53)	
41	(1900 m)	m	[0.33 0.21 −0.38]		124°
		b	[0.05 −0.04 −0.51]	(−0.51)	
		u	[0.00 −0.09 −0.53]	(−0.53)	
		v	[0.00 −0.09 −0.53]	(−0.57)	